Forschungsberichte des

Institutes für Fertigungstechnologie keramischer Bauteile (IFKB)
Herausgeber: o. Prof. Dr. rer. nat. Dr. h.c. mult. Rainer Gadow

Steffen Eßlinger

Additive Fertigung bioaktiver Keramiken zur Herstellung von Knochenersatzstrukturen

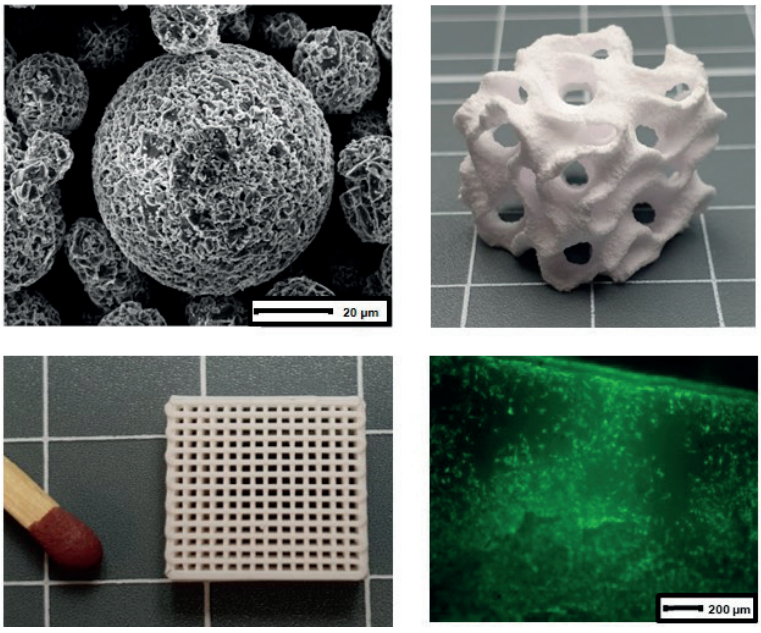

Universität Stuttgart

Graduate School of Excellence advanced Manufacturing Engineering in Stuttgart

Additive Fertigung bioaktiver Keramiken zur Herstellung von Knochenersatzstrukturen

Von der Graduate School of Excellence advanced Manufacturing Engineering

GSaME der Universität Stuttgart

zur Erlangung der Würde eines Doktors der Ingenieurwissenschaften (Dr.-Ing.)

genehmigte Abhandlung

vorgelegt von

Steffen Eßlinger

aus Heilbronn-Neckargartach

Hauptberichter:	o. Prof. Dr. rer. nat. Dr. h.c. mult. Rainer Gadow
Mitberichter:	Prof. Dr. rer. nat Anke Bernstein

Tag der mündlichen Prüfung: 30.06.2020

Institut für Fertigungstechnologie keramischer Bauteile - IFKB

der Universität Stuttgart

2020

Forschungsberichte des Instituts für
Fertigungstechnologie keramischer Bauteile (IFKB)

Steffen Eßlinger

Additive Fertigung bioaktiver Keramiken zur Herstellung von Knochenersatzstrukturen

D 93 (Diss. Universität Stuttgart)

Shaker Verlag
Düren 2020

Bibliografische Information der Deutschen Nationalbibliothek
Die Deutsche Nationalbibliothek verzeichnet diese Publikation in der Deutschen Nationalbibliografie; detaillierte bibliografische Daten sind im Internet über http://dnb.d-nb.de abrufbar.

Zugl.: Stuttgart, Univ., Diss., 2020

Printed in Germany.

ISBN 978-3-8440-7551-9
ISSN 1610-4803

Shaker Verlag GmbH • Am Langen Graben 15a • 52353 Düren
Telefon: 02421 / 99 0 11 - 0 • Telefax: 02421 / 99 0 11 - 9
Internet: www.shaker.de • E-Mail: info@shaker.de

Für meine Eltern, meine Geschwister und Tamara.

Vorwort und Danksagung:

Die vorliegende Dissertationsschrift entstand während meiner Tätigkeit als wissenschaftlicher Mitarbeiter am Institut für Fertigungstechnologie keramischer Bauteile (IFKB) sowie Doktorand der Exzellenzgraduiertenschule *Graduate School of Excellence advanced Manufacturing Engineering* (GSaME) der Universität Stuttgart in den Jahren von 2016 bis 2020.

Mein besonderer Dank gilt Herrn o. Prof. Dr. rer. nat. Dr. h.c. mult. Rainer Gadow für die Ermöglichung der Durchführung des Promotionsvorhabens am IFKB, das mir entgegengebrachte Vertrauen in meine Person und die fachlichen Diskussionen. Darüber hinaus bedanke ich mich dafür, dass ich die Ergebnisse meiner Arbeit auf nationalen und internationalen Tagungen vorstellen konnte und die Möglichkeit hatte, mit anderen Forschungsgruppen zusammen zu arbeiten.

Frau Prof. Dr. rer. nat. Anke Bernstein vom Muskuloskelettalen Forschungszentrum des Universitätsklinikums Freiburg danke ich für die Übernahme des Koreferats, aber vor allem auch für die hervorragende wissenschaftliche Zusammenarbeit in diesem interdisziplinären Forschungsfeld, dem fachlichen Interesse an meiner Arbeit sowie dem freundschaftlichen und kollegialen Umgang.

Herrn apl. Prof. Dr. rer.nat. Frank Kern danke ich für seine Unterstützung und die fachlichen Diskussionen und Anregungen.

Ich möchte mich bei allen Mitarbeitern des IFKB und der GSaME für die gute Zusammenarbeit bedanken. Mein besonderer Dank gilt hierbei Herrn Dr.-Ing. Miguel Jiménez Martínez, Herrn Dr.-Ing. Ulrich Schmitt-Radloff, Herrn Dr.-Ing. Septimiu Popa, Herrn Dr.-Ing. Venancio Martínez Garcia, Herrn Dipl.-Ing. Matthias Blum und Frau Ilia Santoro für die Hilfsbereitschaft und die angenehme Arbeitsatmosphäre auf fachlicher und persönlicher Basis.

Vor allen Dingen möchte ich mich aber bei meiner Familie bedanken: Bei meinen Eltern Martin und Sabine, meiner Schwester Anika und meinem Bruder Tobias für ihren stetigen Rückhalt, Förderung und Unterstützung auf meinem bisherigen Lebensweg. Von ganzem Herzen möchte ich meiner langjährigen Lebenspartnerin Tamara danken, die mir in der Zeit, in der diese Dissertation entstand, viel Liebe, Geduld und Unterstützung entgegengebracht hat.

Stuttgart, im Juli 2020

Steffen Eßlinger

Inhaltsverzeichnis

Formelzeichen

B_S		Bindersättigung
d_{Scaff}	mm	Durchmesser der Scaffolds
E	GPa	Elastizitätsmodul
F_{max}	N	Höchstkraft bei Probenbruch
g	m/s^2	Erdbeschleunigung
HR		Hausnerfaktor
L	mm	Abstand zwischen Extruder und Hotend
n		Brechungsindex
NC		Netzwerkkonnektivität
p	Pa	Druck
Q	mm^2	Querschnittsfläche der Scaffolds
Q_{eff}	mm^2	Effektive Querschnittsfläche der Scaffolds
R	mm	Filamentdurchmesser
Ra	µm	Mittenrauwert
Rz	µm	Gemittelte Rautiefe
r	m	Radius eines Partikels / Porenradius
t	s	Zeit
$V_{Hüll}$	mm^3	Definiertes Hüllvolumen im Pulverbett
$V_{L,ist}$	mm^3	Leervolumen im Pulverbett
$V_{L,soll}$	mm^3	Leervolumen im Pulverbett, das mit Binder gefüllt werden soll
v_s	m/s	Sedimentationsgeschwindigkeit
ε		Porosität
$\dot{\gamma}$	1/s	Schergeschwindigkeit
ρ_D	g/cm^3	Dichte des Dispersionsmediums
ρ_P	g/cm^3	Dichte eines Partikels

ρ_{PB}	g/cm^3	Dichte des Pulverbetts
$\rho_{Schütt}$	g/cm^3	Schüttdichte
ρ_{Stampf}	g/cm^3	Stampfdichte
$\sigma_{krit, knick}$	MPa	Kritische Knickspannung
σ_O	MPa	Oberflächenspannung
τ	MPa	Schubspannung
η	m^2/s	Viskosität
θ	°	Benetzungswinkel

Abkürzungen

ABS	Acrylnitril Butadien Styrol
Al_2O_3	Aluminiumoxid
AM	Additive Manufacturing
BG_C	Bioglas der Firma Colorobbia
BG_S	Bioglas der Firma Schott
BJ	Binder Jetting
bTCP	β-Tricalciumphosphat
.amf	Additive Manufacturing File Format
CAD	Computer Aided Design
CaO	Calciumoxid
DLP	Digital Light Processing
DTA	Differenz-Thermo-Analyse
EBM	Electron Beam Melting
F	Fluor
FDC	Fused Deposition of Ceramics
FDM	Fused Deposition Modelling
FFF	Fused Filament Fabrication
FLM	Fused Layer Modelling
.iges	Initial Graphics Exchange Specification
iSFF	indirect Solid Freeform Fabrication
.jt	Jupiter Tesselation
LCM	Lithography-based Ceramic Manufacturing
LDA	Life-Dead-Assay
MgO	Magnesiumoxid
NaO	Natriumoxid

PEG	Polyethylenglykol
PETG	Glycol modifiziertes Polyethylenterephthalat
PLA	Polylactide Acide, dt: Polymilchsäure
.ply	Polygon File Format
PVA	Polyvinylalkohol
P_2O_5	Phosphorpentoxid
SiC	Siliziumcarbid
SiO_2	Siliziumdioxid
SLM	Selective Laser Melting
SLS	Selective Laser Sintering
.step	Standard for the Exchange of Product Model Data
STL	Stereolithografie
.stl	Standard Triangulation Language (alternative: Standard Tesselation Language)
TG	Thermogravimetrie
.vrml	Virtual Reality Modelling Language
XRD	X-Ray Diffraction

Extended Abstract

Introduction

Experts agree that the additive manufacturing technologies will show a strong growth in industrial manufacturing in the future [WL16]. Especially in the context of digitization and Industry 4.0, additive manufacturing processes are considered to have high potential [Ger17], [Hub18], [Neu18].

The main characteristic of additive manufacturing or simply 3D printing is that the component is build up layer by layer. Compared to conventional manufacturing technologies like milling and turning no shaping tool is required. For this reason, the smallest batch sizes can be manufactured economically using additive manufacturing. Furthermore, components can be produced by means of 3D printing, which, due to their complex shape, would not be possible to produce with conventional methods or only at an increased cost. Nowadays there are varieties of different additive manufacturing technologies. Almost any material, whether plastic, metal or ceramic, can be printed.

One possible field of application in which additive manufacturing can use its strengths is the customized manufacture of bone implants, so called scaffolds. Bones are filigree, complex structures that consist mainly on calcium phosphates and differ from each individual. Nowadays, the autologous bone graft is considered as the gold standard [HOH18]. With this strategy, the patient's own tissue is removed and implanted again at the required location. These implants are well tolerated. However, the amount of suitable bone available is small and the operations are very painful for the patient. The use of 3D printed implants would therefore be advantageous for the treatment of the patient, especially since the implant materials are available in almost unlimited quantities. In addition, the cost benefits for healthcare should not be overlooked: The German Society for Orthopedics and Trauma Surgery (DGOU) states that diseases of the musculoskeletal system cause more than 20% of the direct and more than 40% of the indirect national healthcare costs. Four of ten of all sick days are due to such diseases [NS12]. 3D printed implants based on advanced high performance bioceramics can reduce the number of surgeries and restore health overall faster. Therefore, bioactive glasses and calcium phosphate ceramics can be used. If these ceramics are processed into highly porous, complex structures by means of additive manufacturing, then osteoconductive and -inductive implants can be manufactured that stimulate bone growth and after a while are converted into the body's own tissue. Before such implants become standard, however, a lot of research has to be invested in materials technology and the additive manufacturing process.

Aims of this work

In the present work, the preparation and processing of high performance bioceramics is examined. The investigations encompass the entire ceramic production chain, from the powder to the shaping to the sintered component. First, the starting powders must be converted into suitable suspensions. To do this, rheological tests must be carried out and the most important liquefaction parameters identified. The suspensions have to be developed in such a way that the powder can be ground, but also granules with customized properties during spray drying can be received. Furthermore, the suspensions must be usable as pouring slurries and allow complete mold filling. The bioceramics prepared in this way are then processed into complex three-dimensional structures using additive manufacturing. The optimal printing parameters must be identified so that the printed components meet the most important medical requirements for artificial bone grafts. Since ceramic components only get their final properties through the sintering process, extensive thermal analyzes for debinding and sintering of the printed components must be carried out. In the end, the ceramic components should meet the requirements for bone replacement structures:

- sufficient strength in the order of cancellous bone
- highest possible porosity and roughness of the surface to ensure cell growth and multiplication as well as their supply with nutrients
- filigree structures similar to human bones
- biocompatibility and bioactivity
- reproducible component quality
- economic processability of the bioceramic starting powder

All process steps are accompanied by extensive analyzes. The biocompatibility and activity is determined in vitro using cell tests carried out by the university hospital of Freiburg.

Materials and methods

In this work, scaffolds are manufactured by different additive manufacturing technologies:

- powder-based Binder Jetting
- filament-based indirect Solid Freeform Fabrication (iSFF) using Fused Deposition Modelling (FDM) printers in combination with ceramic slip casting
- filament-based Fused Deposition of Ceramics (FDC)

The bioceramics used are β-tricalcium phosphate and bioactive glass. The chemical composition of the glass is similar to henchglas or 45S5.

The raw materials must be processed for the shaping via additive manufacturing. For the Binder Jetting spherical granules with a medium particle size of 35 – 50 µm are required. Therefore the bioceramics are processed into slurries, milled and spray granulated using a spray drying tower. For the printing a ZPrinter 510 Plus (ZCorporation, USA) is used.

The filament-based printing FDC and iSFF are carried out with a FDM printer Prusa i3 MK3 and Prusa i3 MK3S, respectively. For the iSFF approach thermoplastic lost forms are printed that represent the negative of the scaffold geometry. The suspensions are adjusted to fill the mold in order to be as low-viscosity as possible. The infill is taken place on a porous gypsum board, as it is used for conventional slip casting. The filaments for FDC were compounded and extruded in cooperation with the Institut für Kunststofftechnik (IKT) at the University of Stuttgart.

The debinding and sintering is one of the most important steps in the manufacturing of the 3D printed scaffolds. Therefore the thermal behavior of the components is investigated by combined thermal analysis methods.

The investigation on the biocompatibility and –activity is done in vitro via life-dead-assays by the University Hospital of Freiburg.

The process steps as well as the printed scaffolds are analyzed using the following methods:

- laser granulometry
- rheology measurements
- optical analysis (optical microscopy and SEM-images)
- differential thermal analysis
- thermogravimetric analysis
- compressive strength measurements
- mercury intrusion porosimetry

Results and Discussion

In this chapter the most important results are presented for the three different manufacturing strategies used in this work.

Scaffold manufacturing via Binder Jetting

The bioglass powders as well as the β-tricalcium phosphates (bTCP) were dispersed in water using different dispersants. For the following process of spray granulation a shear-thinning behavior and a high solid content was necessary. The bioglass suspensions were all shear thinning. The bTCP suspensions were shear-thickening at shear rates over 10 s^{-1}. The maximum amount for the bioglass suspensions was 65 wt-%, which is a volume content of 40 vol-

%, the maximum solid content bTCP within the suspensions was 70 wt_%, which is a volume content of 41 vol-%.

After spray granulation all powders showed a spherical morphology and a perfect particle size between 31 – 50 µm. SEM images of the spray dried powders are shown in Figure 1.

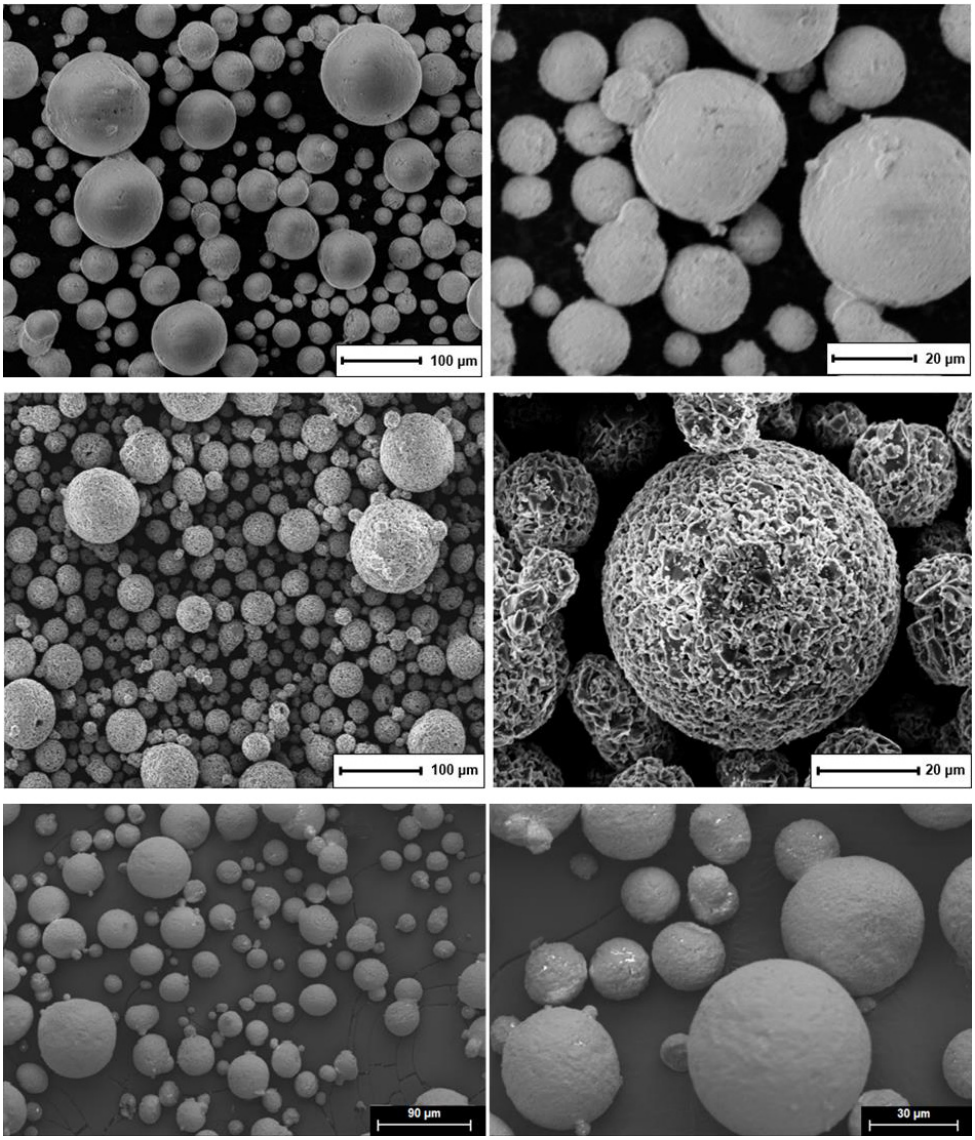

Figure 1: SEM images of spray granulated bioceramics. Top and middle: bioglass; bottom: bTCP

The bioglass powder was either ground until the medium particle size was smaller than 1 µm, see Figure 1, top, or not grinded and spray dried immediately, see Figure 1, middle. The SEM-

images in Figure 1, bottom shows the spray granulated bTCP, which was also ground until the medium particle size was smaller than 1 µm.

The printing parameters were investigated. In general one can say, that the compressive strength of the green parts as well as the sintered scaffolds increases with higher saturation values and smaller layer thickness. The bioglass samples tested were sintered at 950 °C for 4 h, the bTCP samples at 1250 °C for 4 h. bTCP cylinders had a maximum compressive strength of 7.52 ± 0.34 MPa, the bioglass scaffolds had a maximum compressive strength of 5.43 ± 1.70 MPa. The bTCP scaffolds reached maximum values of 7.52 ± 0.34 MPa. The compressive strength is similar to cancellous bone. A picture of the tested scaffolds is shown in Figure 2.

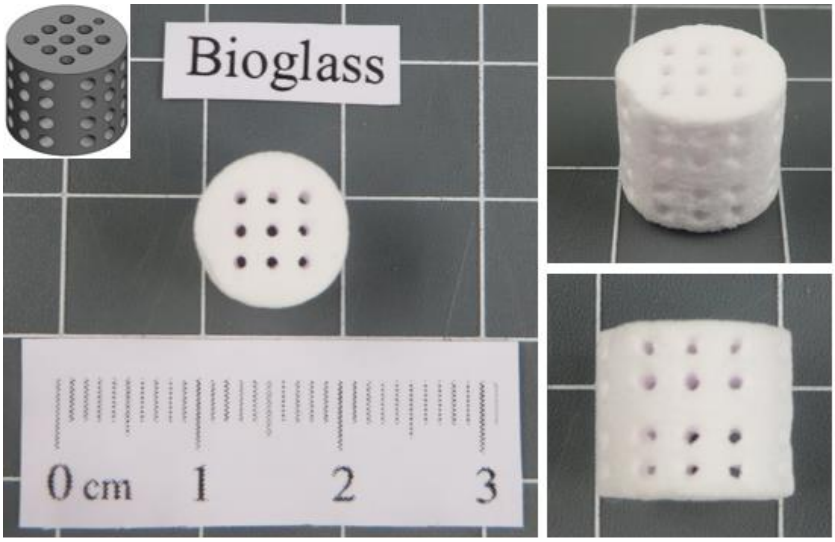

Figure 2: Sintered bioglass scaffolds

The porosity of the bioglass samples was 47 % with a medium pore size of 5.8 µm, the porosity of the bTCP samples was 52 % with a medium pore size of 11.2 µm.

The biocompatibility was tested in vitro via life-dead-assay. The tested scaffolds enabled the ingrowth of cells and their proliferation.

Scaffold manufacturing via iSFF

The printed molds consisted of thermoplastics, ABS, PETG and PLA. The slurries showed a lower viscosity than the ones used for spray granulation. This was reached by decreasing the solid content. The maximum solid content for the bioglass slurries was 60 wt-%, which is a volume content of 35 vol-%. The bTCP slurries contained 65 wt-% and 36 vol-%, respectively.

The smallest pore size that could be created was 0.25 mm for PLA molds and 0.5 mm for ABS and PETG molds. The bTCP slurries could be casted in every kind of thermoplastic. The combination of bioglass and PLA led to a foaming reaction and the destruction of the scaffold. The results of the thermal analysis for the debinding of pure PLA, bioglass and PLA and bTCP and PLA are shown in Figure 3.

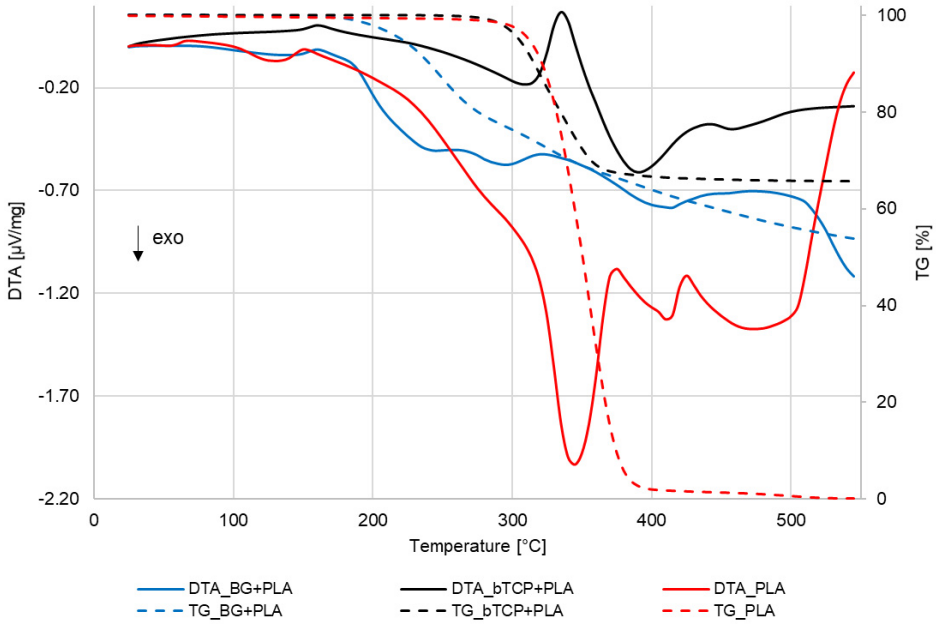

Figure 3: DTA/TG for different combinations of bioceramics and PLA

Compared to the Binder Jetting technique the consolidation of the ceramic particles was higher. This is caused by capillary forces during the casting process on the porous plaster mould. For this reason the maximum sintering temperature for the bioglass samples could be lowered to 750 °C. The bTCP scaffolds were sintered identically like the ones printed via Binder Jetting.

The maximum strength of the bioglass scaffolds was 18.86 ± 2.32 MPa, the maximum strength for the bTCP scaffolds 17.23 ± 2.03 MPa. In addition, the porosity was significantly lower, 40 %

for the bioglass samples with a medium pore size of 0.4 µm. The porosity of the bTCP samples was 16 %, the pore size distribution 1 µm. The strength is higher than cortical bone, the lower density is a disadvantage compared to the Binder Jetting scaffolds.

Microscopy pictures showed, that there are often cracks near the area where the thermoplastic struts were in the green bodies, see Figure 4. Despite, the compressive strength was higher than the Binder Jetting Scaffolds that had no cracks within the microstructure. The cracks and the formerly thermoplastic layers can be seen in Figure 4.

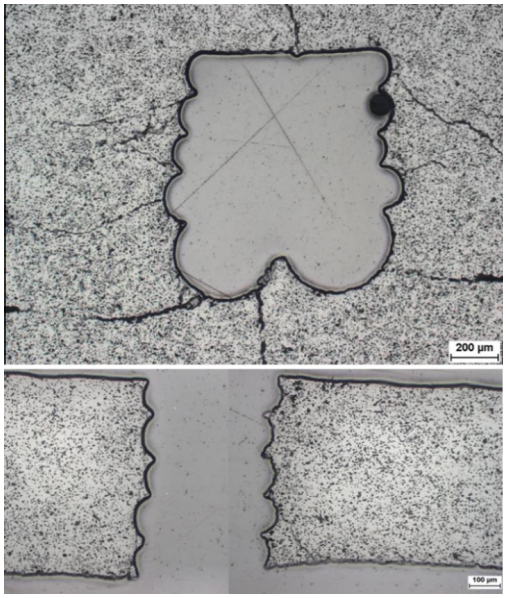

Figure 4: Grinding patterns of a sintered bioglass scaffold

Scaffolds as shown in Figure 5 were tested via Life-Dead-Assay. The scaffolds showed high biocompatibility, which can be concluded by the green fluorescence of the living cells, see Figure 6.

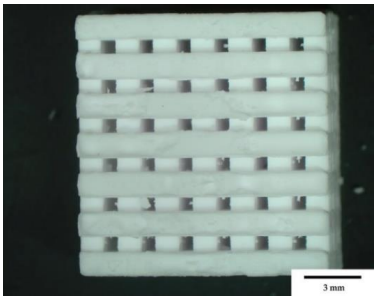

Figure 5: Sintered bTCP scaffold with pore sizes of 0.5 mm for testing via life-dead-assay [SLE19]

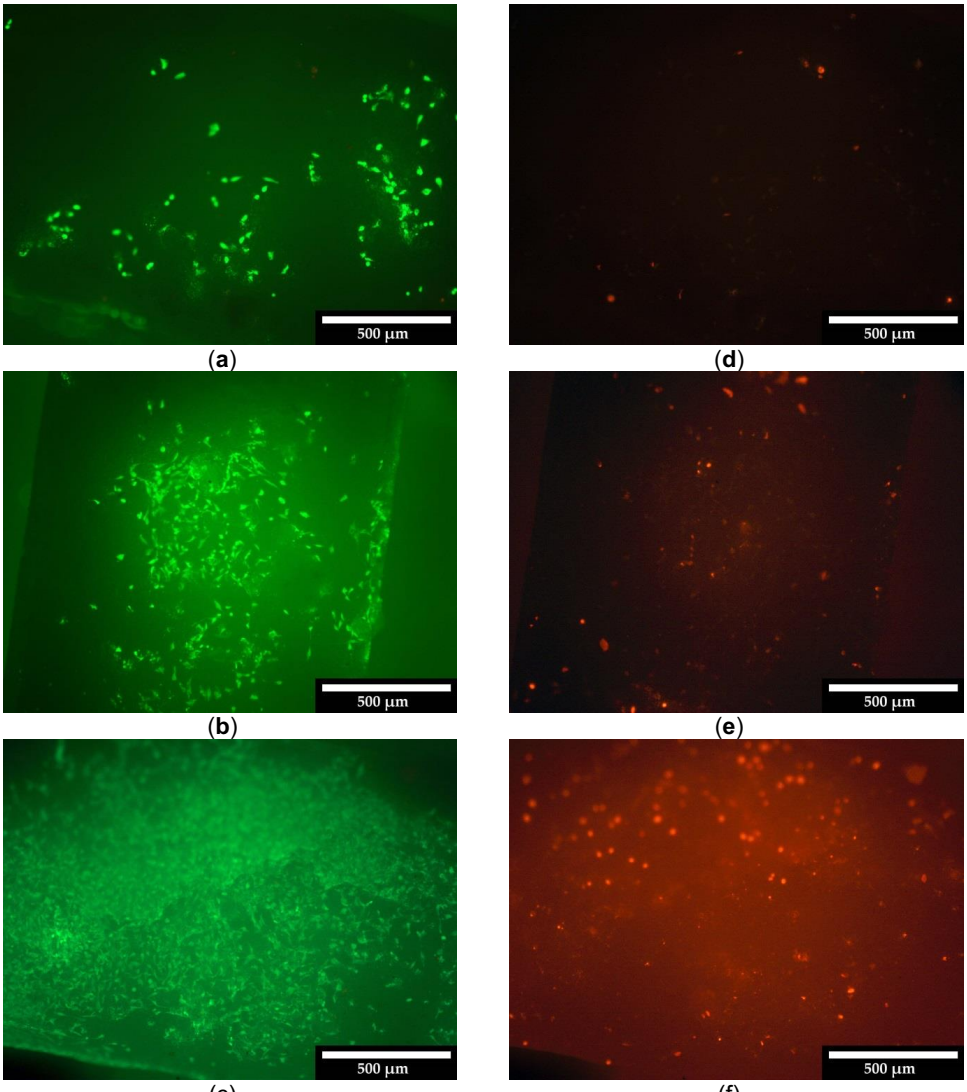

Figure 6: Living cells (left pictures) and dead cells (right pictures) on bTCP scaffold after 3 days (a, d), 7 days (b, e) and 10 days (c, f)

Scaffold manufacturing via FDC

The compounded filaments contained different amounts of bTCP. Organic additives were PLA and PEG. The filaments showed a homogeneous distribution of the ceramic powders in the filament, see Figure 7.

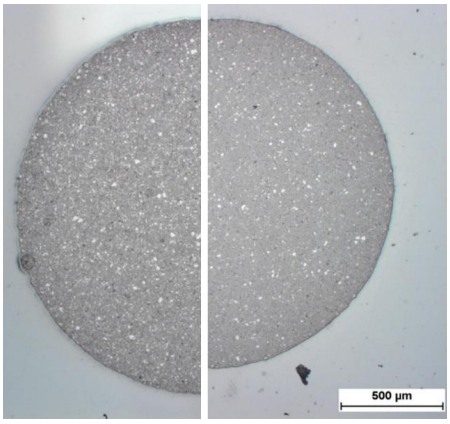

Figure 7: bTCP distribution in the PLA filament with a n diameter of 1,75 ± 0,2 mm

The filaments could be printed with a commercial FDM printer Prusa i3 MK3. Depending on the component geometry, the printing parameters had to be heavily adjusted. A picture of a printed bTCP-PLA scaffold can be seen in Figure 8 as well as the grinding pattern showing the distribution of the ceramic particles within the sample.

The higher the amount of water soluble PEG, the lower the printing quality. Without the use of PEG a debinding of the printed structures was not possible. For the debinding the PEG was solved in a water bath for 72 h, then the PLA was thermally debindered. During the debinding the green body was inserted into an alumina powder bed. With this strategy the samples could be debindered and sintered without damaging the component. Compared to the other scaffolds printed via Binder Jetting or iSFF approach, the quality was extremely low, see Figure 9.

Figure 8: bTCP-PLA green body after printing and grinding pattern

Figure 9: Debindered and sintererd bTCP scaffolds. The scaffold on the left was debindered without a powder bed

Summary and Conclusion

It can be summarized, that the main goals of this work are accomplished. The bioceramic raw materials were successfully processed for the additive manufacturing process. Scaffolds could be printed, debindered and sintered without damaging the components. The properties of the sintered scaffolds fulfilled most of the requirements for artificial bone grafts: filigree structures with high porosity and mechanical strength similar to human cortical bone. Cell tests in vitro indicated the biocompatibility of the scaffolds and made cell growth possible.

For future investigations, the osteoconductive properties of the 3D printed scaffolds should be tested in vivo. The quality of the FDC scaffolds must be improved and further research on the bioglass materials should be done.